SOLUTION OF WAVE EQUATIONS NEAR SEAWALLS BY FINITE ELEMENT METHOD

S. A. Mirbagheri* and T. Rajaee

Department of Civil Engineering, K.N. Toosi University of Technology
P.O. Box 15875-4416, Tehran, Iran
mirbagheri@kntu.ac.ir - rajaee@alborz.kntu.ac.ir

F. Mirzaee

Department of Civil Engineering, Shiraz University
Shiraz, Iran

*Corresponding Author

(**Received: October 1, 2006 – Accepted in Revised Form: September 13, 2007)**

Abstract A 2D finite element model for the solution of wave equations is developed. The fluid is considered as incompressible and irrotational. This is a difficult mathematical problem to solve numerically as well as analytically because the condition of the dynamic boundary (Bernoulli's equation) on the free surface is not fixed and varies with time. The finite element technique is applied to solve nonlinear wave equations. The finite element model includes the conventional method based on a variational principle. This model minimizes the relevant function of the problem. After calculating two independent variables (i.e. ϕ and η) the pressure, forces and moments acting on sea-walls can be computed. These values are compared with existing experimental and theoretical outputs. The standing wave behavior is well described by the model, e.g. we can get the envelope of breaking waves in curve designs, which are developed for non-breaking waves. Also we can estimate the effective depth of a certain wave. Therefore the model can be used to propose some design curves.

Keywords Finite Element Method, Wave Equation, Seawalls, Numerical Method

چکیده در این مقاله یک مدل دوبعدی اجزای محدود برای حل معادلات موج ارائه شده است. سیال بصورت غیرقابل تراکم و غیرچرخشی در نظر گرفته شده است. حل این مساله بدلیل وجود شرایط مرزی دینامیکی (معادله برنولی) در سطح آزاد، مشکل است زیرا این یک شرط غیر خطی بوده و مکان سطح آزاد در ابتدا مشخص نیست. در این تحقیق، روش المان محدود برای حل معادلات غیر خطی موج بکار گرفته شده است. روش المان محدود استفاده شده بر پایه اصول تغییراتی می‌باشد. بعد از بدست آوردن دو متغیر مستقل ϕ و η، نیروهای فشاری و لنگرهای خمشی ایجاد شده بر روی دیواره محاسبه می‌شوند. در ادامه، مقادیر محاسبه شده با نتایج آزمایشگاهی و نیز نتایج تحقیقات نظری مقایسه شده اند. نتایج نشان دهنده قابلیت مدل در مدل سازی رفتار امواج ایستاده می باشد، بطوریکه می توان پوش امواج شکسته شده را در منحنی های مربوط به امواج شکسته نشده رسم کرد و یا می‌توان عمق اثر یک موج مشخص را تعیین نمود. همچنین مدل قادر به ارائه منحنی های طراحی می‌باشد.

1. INTRODUCTION

One of the main problems in the analysis of wave effects on marine structures is to approximate the forces acting on sea-walls. Unfortunately, there is no explicit formula for calculating these forces and their momentums.

A good understanding of the behavior of an off-shore structure depends on a good understanding of the surrounding wave fields and relevant forces. In other words, the main step in loading such structures is to solve the wave field around them.

The literature review on this subject suggests that a number of wave crests are parallel to the wall so that the reflection effect can be ignored [1].

Therefore, it will be enough to analyze only the effect of a standing wave on the wall. It is supposed that the maximum pressure load on the wall occurs in such case; however this has been shown that the ultimate pressure belongs to the waves that strikes the wall obliquely and then reflects back.

One of the most important problems in fluid mechanics is the analysis of nonlinear behavior of a fluid with a free surface. Evidently, such problems are numerically-analytically troublesome. This difficulty is caused by dynamic boundary condition (Bernoulli equation) at free-surface, where the location of free surfaces is time dependent and may or may not be initially determined.

Although several investigations are conducted with this theory never the less, there are many problems left for the future. In this paper a finite element model is developed to solve the wave equations near seawalls. This includes the conventional methods based on variational principles.

2. GOVERNING EQUATIONS AND BOUNNDARY CONDITIONS

Assuming the flow is incompressible and irrotational, the Laplace equation defines the problem over the flow domain:

$$\frac{\partial^2 \phi}{\partial x^2} + \frac{\partial^2 \phi}{\partial y^2} = 0 \tag{1}$$

With four boundary conditions:

$$\frac{\partial \phi}{\partial y} = 0 \quad \text{at} \quad y = -h \tag{2}$$

$$\frac{\partial \eta}{\partial t} + \frac{\partial \phi}{\partial x}\frac{\partial \eta}{\partial x} - \frac{\partial \phi}{\partial y} = 0 \quad \text{at } y = \eta \tag{3}$$

$$\frac{\partial \phi}{\partial t} + \frac{1}{2}\left[(\frac{\partial \phi}{\partial x})^2 + (\frac{\partial \phi}{\partial y})^2 \right] + g\eta = 0 \quad \text{at} \quad y = \eta \tag{4}$$

$$\phi(x, y, t) = \phi(x - ct, y) \tag{4a}$$

$$\frac{\partial \phi}{\partial x} = 0 \qquad \text{at } x = 0 \tag{5}$$

Where X and Y are horizontal and vertical coordinate, h is the mean water level and $\eta(x,t)$ states the location of free surface above the still water level. Equation 2 sets the horizontal velocity component to be zero at bottom. Equations 3 and 4 state the kinematic and dynamic boundary conditions at free surface, respectively. Equation 3 also indicates that the fluid particles just in contact with free surface will remain in contact with it. The dynamic boundary condition states the iso-pressure free surface (which is set to be zero in Bernoulli equation). This equation stands where the surface tension is neglected. The velocities at vertical boundaries are set to be zero in Equation 5.

Now what is left is to find the potential function ϕ and to compute the desired forces and moments. Figure 1 shows the geometry, the boundary conditions and also the direction of the wave.

2.1. Literature Review of Existing Methods

The problem of a standing wave with zero contact angle is analyzed by Tadjbaksh, et al [2]. Goda [3] has analyzed the same problem using fourth order approximation. He studied the pressure of standing waves in more details. Sainflous, et al [4] found that in the case of high amplitude waves where the water is deep enough, for most cases the maximum pressure occurs near the wave crest, not just at maximum.

Tsuchiya, et al [5] made a comparison between various analytical methods and experimental data and observed that the first and second order theories stand over limited ranges while the third and fourth order theories agree with a large domain of experiments.

Nagai [1] made a comparison between experimental data and irrational theories and

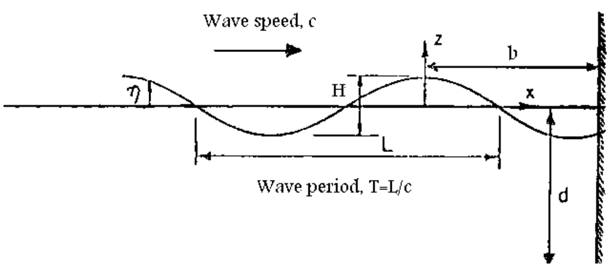

Figure 1. General form of the wave on the seawall.

developed relations for maximum applicable pressure. In case of inclining reflected waves, the intersecting waves are a kind of short-crested waves in which the top view of intersections has regularly, repeated diamond-like appearance.

The common theoretical method for the solution of short-crested waves is the Stokes theory, which is applicable for deep waters. Hsu, et al [6], developed the third order method. Roberts [7] and Roberts, et al [8] studied the problems in more details. Using Fourier expansion they developed numerical approximation to higher orders.

While the forces and the moments are matters of interest, none of the above mentioned papers had studied the parameters of the force. Battjes [9] developed expressions based on the linear theory for intersecting short- crested waves. Clark [10] solved the three dimensional wave problems for off-shore structures using frequency domain method. In the same year, Liao [11] developed the solitary wave equations using finite process method. Cao [12] studied the solitary waves generated by ship motion. Cao, et al [13] analyzed the solitary waves generated by submarines and moving objects. Johnson [14] simulated the impact of wave on solid boundaries. Takikawa [15] used the model developed by Washisu to study the wave effect on floating bodies.

2.2. Finite Element Model This model was first used by Washizu [16] for slashing problem in wave tanks. The model used the variational technique to minimize the relevant function of the problem.

This kind of problem can be defined by the following equation:

$$\int_{\Omega} G_j(u)d\Omega + \int_{\Gamma} g_j(u)d\Gamma = 0 \tag{6}$$

In which G_j and g_j are the specific function that can be integrated. The Equation 6 can be changed in the form:

$$\int_{\Omega} G_j(u)d\Omega + \int_{\Gamma} g_j(u)d\Gamma = \sum_{e=1}^{m} \left(\int_{\Omega^e} G_j(u)d\Omega + \int_{\Gamma^e} g_j(u)d\Gamma \right) \tag{7}$$

In which Ω is the domain element and Γ is the boundary.

For the application of finite element method to solve this kind of problem, first the variational method is used in the following equation:

$$\Pi = \int_{\Omega} F\left(u, \frac{\partial u}{\partial x}, ...\right) d\Omega + \int_{\Gamma} E\left(u, \frac{\partial u}{\partial x}, ...\right) d\Gamma \tag{8}$$

In which u is the unknown function, E and F are specific operators.

Luck [17] has stated this variational principle as below:

$$x = I_1 + I_2 + I_3 + I_4 \tag{9}$$

$$I_1 = \frac{1}{2} \iint_{V(\eta)} \left\{ \left(\frac{\partial \phi}{\partial x}\right)^2 + \left(\frac{\partial \phi}{\partial y}\right)^2 \right\} dxdy \tag{10}$$

$$I_2 = \frac{1}{2} \int_0^{\infty} g\eta^2 \, dx \tag{11}$$

$$I_3 = \int_0^{\infty} \frac{\partial \phi}{\partial t} \eta dx \tag{12}$$

$$I_4 = -\int_0^{\infty} \frac{\partial \eta}{\partial t} \phi dx \tag{13}$$

In which ϕ and η are independent variables of variational expression. Note that the fluid volume V acts as a function of η. Also $\frac{\partial \phi}{\partial t}$ and $\frac{\partial \eta}{\partial t}$ are assumed to be constant during the time increment Δ; so their first order variations are neglected in each element as shown in Figure 2, the parameter ϕ is specified as a linear function of x and y:

$$\phi = a + bx + cy \tag{14}$$

The function η on the boundary is defined as a

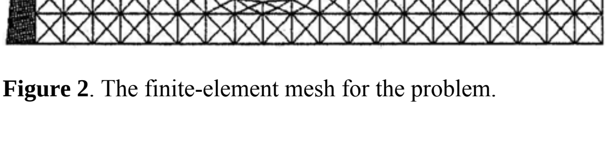

Figure 2. The finite-element mesh for the problem.

product of isoperimetric functions as below:

$$\eta = \frac{1}{2}(1-r)\eta_i + \frac{1}{2}(1+r)\eta_k \tag{15}$$

After each time increment, the unknown values of the problem are considered to have the form of:

$$\phi = \phi_0 + \Delta\phi \ , \ \eta = \eta_0 + \Delta\eta \qquad \text{at} \quad t = t_0 + \Delta t \tag{16}$$

Where ϕ_0 and η_0 are the values obtained in previous step. Considering Figure 3 and regarding back to Equation 14, for the time t_0 it can be written that:

$$\frac{\partial\phi}{\partial x} = A_0^T \phi = b = \text{cnst} \tag{17}$$

$$\frac{\partial\phi}{\partial y} = B_0^T \phi = c = \text{cnst} \tag{18}$$

$$B_0^T = \frac{1}{2\Delta_0}[X_k - X_j, X_i - X_k, X_j - X_i] \tag{19}$$

$$\phi_0^T = \left[\phi_{0_i}, \phi_{0_j}, \phi_{0_k}\right] \tag{20}$$

After each tie increment, the area of the triangle $p_i p_j p_k$ is:

$$\Delta = \Delta_0 + P^T \Delta\eta \tag{21}$$

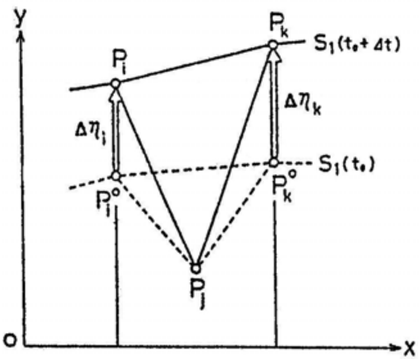

Figure 3. The element in contact with upper boundary.

Where $\Delta\eta$ represents the vector of unknowns and Δ_0 and P contains the known values of pervious step:

$$P^T = \frac{1}{2}\left[X_K - X_j, X_i - X_K, X_j - X_i\right] \tag{22}$$

$$\Delta\eta^T = \left[\Delta\eta_i, 0, \Delta\eta_K\right] \tag{23}$$

Also:

$$\frac{\partial\phi}{\partial x} = A_0^T\left\{\phi_0 + \Delta\phi\right\} + \Delta\eta^T A_1^T \ \phi_0 \tag{24}$$

$$\frac{\partial\phi}{\partial x} = [A_0 + A_1 \Delta\eta]^T \{\phi_0 + \Delta\phi\} \tag{25}$$

$$A_1 = \frac{1}{(2\Delta_0)^2}$$

$$\begin{bmatrix} (y_j - y_k^0)(x_k - x_j) & 0 & 2\Delta_0 + (y_j - y_k^0)(x_j - x_i) \\ 2\Delta_0 + (y_k^0 - y_i^0)(x_k - x_j) & 0 & -2\Delta_0 + (y_k^0 - y_i^0)(x_j - x_i) \\ -2\Delta_0 + (y_i^0 - y_j)(x_k - x_j & 0 & (y_i^0 - y_j)(x_j - x_i) \end{bmatrix} \tag{26}$$

$$\frac{\partial\phi}{\partial y} = B_0^T\{\phi_0 + \Delta\phi\} + \Delta\eta^T B_1^T \phi_0 \tag{27}$$

$$\frac{\partial\phi}{\partial y} = [B_0 + B_1 \Delta\eta]^T \{\phi_0 + \Delta\phi\} \tag{28}$$

$$B_1 = \frac{1}{(2\Delta_0)^2}$$

$$\begin{bmatrix} (x_k - x_j)^2 & 0 & (x_k - x_j)(x_j - x_i) \\ (x_k - x_j)(x_i - x_k) & 0 & (x_i - x_k)(x_j - x_i) \\ (x_k - x_j)(x_j - x_i) & 0 & (x_j - x_i)^2 \end{bmatrix} \tag{29}$$

Now, substituting each of variables in the variational expression, leads to:

$$I_1 = \frac{1}{2}\iint \{b^2 + c^2\} dxdy \tag{30}$$

$$I_1 = \frac{1}{2}\sum_e \{\phi_0 + \Delta\phi\}^T \{[A_0 + A_1\Delta\eta][A_0{}^T + \Delta\eta^T A_1{}^T] + [B_0 + B_1\Delta\eta][B_0{}^T + \Delta\eta^T B_1{}^T]\}\{\phi_0 + \Delta\phi\}\left(\Delta_0 + P^T\Delta\eta\right) \quad (31)$$

Also Equation 11 can be computed as bellow:

$$I_2 = \frac{1}{2} g \sum_{se} \{\eta\}^T F\{\eta\} \quad (32)$$

$$I_2 = \frac{1}{2} g \sum_{se} \{\eta_0 + \Delta\eta\}^T F\{\eta_0 + \Delta\eta\} \quad (33)$$

$$F = \frac{l}{6}\begin{bmatrix} 2 & 1 \\ 1 & 2 \end{bmatrix} \quad (34)$$

Where l represents the horizontal length of the element on the boundary S_1, for example $l = x_i - x_k$ in Figure 4. Since the isoperimetric functions are used for all variables over the boundary, for the variational term I_3 it can be shown that:

$$\frac{\partial\phi}{\partial t} = \frac{1}{2}(1-r)(\frac{\partial\phi}{\partial t})_i + \frac{1}{2}(1+r)(\frac{\partial\phi}{\partial t})_k \quad (35)$$

$$I_3 = \sum_{se} \int_{-1}^{+1} \{\eta\}^T \begin{Bmatrix} \frac{1-r}{2} \\ \frac{1+r}{2} \end{Bmatrix} \begin{bmatrix} \frac{1-r}{2} & \frac{1+r}{2} \end{bmatrix} \begin{Bmatrix} \frac{\partial\phi}{\partial t} \end{Bmatrix} \quad (36)$$

$$I_3 = \sum_{se} \{\eta\}^T F \begin{Bmatrix} \frac{\partial\phi}{\partial t} \end{Bmatrix} \quad (37)$$

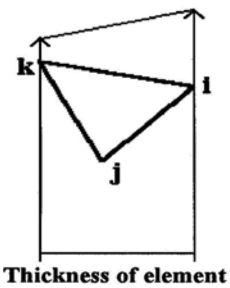

Figure 4. Variation of η with respect to x.

$$I_3 = \sum_{se} \{\eta_0 + \Delta\eta\}^T F \begin{Bmatrix} \frac{\partial\phi}{\partial t} \end{Bmatrix} \quad (38)$$

Also the parameters $\frac{\partial\eta}{\partial t}$ and ϕ over the boundary may be shown as:

$$\frac{\partial\eta}{\partial t} = \frac{1}{2}(1-r)(\frac{\partial\eta}{\partial t})_i + \frac{1}{2}(1+r)(\frac{\partial\eta}{\partial t})_k \quad (39)$$

$$\phi = \frac{1}{2}(1-r)\phi_i + \frac{1}{2}(1+r)\phi_k \quad (40)$$

Then:

$$I_4 = -\sum_{se} \int_{-1}^{+1} \{\phi\}^T \begin{Bmatrix} \frac{1-r}{2} \\ \frac{1+r}{2} \end{Bmatrix} \begin{bmatrix} \frac{1-r}{2} & \frac{1+r}{2} \end{bmatrix} \begin{Bmatrix} \frac{\partial\eta}{\partial t} \end{Bmatrix} \quad (41)$$

$$I_4 = -\sum_{se} \{\phi\}^T F \begin{Bmatrix} \frac{\partial\eta}{\partial t} \end{Bmatrix} \quad (42)$$

$$I_4 = -\sum_{se} \{\phi_0 + \Delta\phi\}^T F \begin{Bmatrix} \frac{\partial\eta}{\partial t} \end{Bmatrix} \quad (43)$$

Finally, the variational expression has the form of:

$$x = \frac{1}{2}\sum_e \{\phi_0 + \Delta\phi\}^T \{[A_0 + A_1\Delta\eta][A_0^T + \Delta\eta^T A_1^T] + [B_0 + B_1\Delta\eta][B_0^T + \Delta\eta^T B_1^T]\}\{\phi_0 + \Delta\phi\}\left(\Delta_0 + P^T\Delta\eta\right) + \frac{1}{2} g \sum_{se} \{\eta_0 + \Delta\eta\}^T F\{\eta_0 + \Delta\eta\} + \sum_{se} \{\eta_0 + \Delta\eta\}^T F \begin{Bmatrix} \frac{\partial\phi}{\partial t} \end{Bmatrix} - \sum_{se} \{\phi_0 + \Delta\phi\}^T F \begin{Bmatrix} \frac{\partial\eta}{\partial t} \end{Bmatrix} \quad (44)$$

Having $\Delta\phi$ and $\Delta\eta$ and the variables, the variation of above expression with respect to the variables gives:

$$\delta x = \frac{1}{2}\sum_e \delta\Delta\phi^T [(A_0 A_0{}^T + B_0 B_0{}^T)\phi_0\Delta_0 + \{(A_0{}^T\phi_0 I + A_0\phi_0^T)A_1 + (B_0{}^T\phi_0 I + B_0\phi_0^T)B_1\}\Delta_0\delta\eta$$

$$+(A_0A_0{}^T+B_0B_0{}^T)\Delta\phi\Delta_0+$$
$$(A_0A_0{}^T+B_0B_0{}^T)\phi_0P^T\Delta\eta]+$$
$$\frac{1}{2}\sum_e\delta\Delta\eta^TP\{\phi_0(A_0A_0{}^T+B_0B_0{}^T)\phi_0$$
$$+2\phi_0{}^T(A_0\phi_0^TA_1+B_0\phi_0^TB_1)\Delta\eta+$$
$$2\phi_0{}^T+(A_0A_0{}^T+B_0B_0{}^T)\Delta\phi\}$$
$$+g\sum_{se}\delta\Delta\eta^T(F\eta_0+F\Delta\eta)+$$
$$\sum_{se}\delta\Delta\eta^TF\left\{\frac{\partial\phi}{\partial t}\right\}-\sum_{se}\delta\Delta\phi^TF\left\{\frac{\partial\eta}{\partial t}\right\} \tag{45}$$

In which I indicates the unique matrix. Now Equation 45 leaves a system of linear equations which are really the stability conditions for x with respect to $\Delta\phi$ and $\Delta\eta$, i.e.

$$\frac{\delta x}{\delta\Delta\phi}=0 \tag{46}$$

$$\frac{\delta x}{\delta\Delta\eta}=0 \tag{47}$$

Also $\frac{\partial\phi}{\partial t}$ and $\frac{\partial\eta}{\partial t}$ can be assumed to vary as linear functions of time during the time step Δt. Therefore, where the average slope of beginning and end points of each time step is defined as $\frac{\Delta\phi}{\Delta t}$, it can be shown that:

$$\frac{\partial\phi}{\partial t}=\frac{2}{\Delta t}\Delta\phi-(\frac{\partial\phi}{\partial t})_0 \tag{48}$$

$$\frac{\partial\eta}{\partial t}=\frac{2}{\Delta t}\Delta\eta-(\frac{\partial\eta}{\partial t})_0 \tag{49}$$

Replacing these equations in 45 and satisfying the stability conditions 46 and 47, leads to:

$$[K]\{\Delta u\}=\{R\} \tag{50}$$

$$\begin{bmatrix}G_{11} & G_{12}\\ G_{21} & G_{22}\end{bmatrix}\begin{Bmatrix}\Delta\phi\\ \Delta\eta\end{Bmatrix}=\begin{Bmatrix}R_1\\ R_2\end{Bmatrix} \tag{51}$$

In which:

$$G_{11}=(A_0A_0{}^T+B_0B_0{}^T)\Delta_0$$
$$G_{12}=\{(A_0{}^T\phi_0I+A_0\phi_0^T)A_1+(B_0{}^T\phi_0I+B_0\phi_0^T)B_1\}\Delta_0$$
$$+(A_0A_0{}^T+B_0B_0{}^T)\phi_0P^T-\frac{2}{\Delta t}F$$
$$G_{21}=P\phi_0^T(A_0A_0{}^T+B_0B_0{}^T)+\frac{2}{\Delta t}F$$
$$G_{22}=P\phi_0^T(A_0\phi_0^TA_1+B_0\phi_0^TB_1)+gF$$
$$R_1=-(A_0A_0{}^T+B_0B_0{}^T)\phi_0\Delta_0-F\left\{\frac{\partial\eta}{\partial t}\right\}_0$$
$$R_2=-\frac{1}{2}P\phi_0^T(A_0A_0{}^T+B_0B_0{}^T)\phi_0-gF\phi_0\left\{\frac{\partial\phi}{\partial t}\right\}_0 \tag{52}$$

Solving Equation 51 and replacing $\Delta\phi$ and $\Delta\eta$ in 17, the values of ϕ and η can be obtained for that time step. The same Procedure may be repeated for achieving the dynamic response of the fluid.

2.3. Initial Values The statement 52 includes

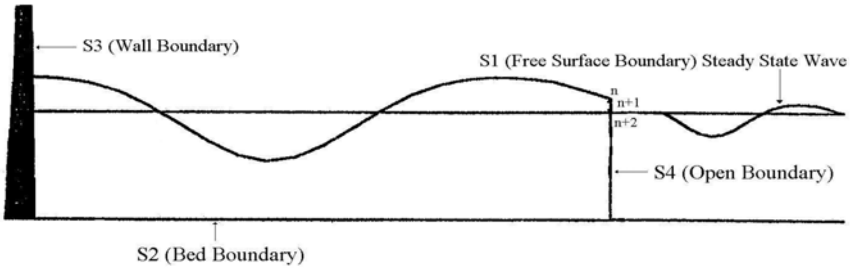

Figure 5. The situation of open boundary.

the initial values of ϕ_0, η_0, $(\frac{\partial\phi}{\partial t})_0$ and $(\frac{\partial\eta}{\partial t})_0$. To define the initial values for the program, it is assumed that the wave comes near the wall as shown in Figure 5. It is assumed that at the spacing b from the wall, the disturbance caused by the wave is eliminated and the wave has a fixed shape. Therefore it can be assumed that in each time step the values of ϕ and η over the boundary S_4 are constant $\Delta\phi$ and $\Delta\eta$ are zero.

At the first step of program execution, the values of ϕ_0 and η_0 are considered to be zero, except for the boundary S_4, on which the above variables are constant for each time step. To evaluate these values, the specifications of a short-crested wave are considered. As it is shown in Figure 5, just at the beginning of execution, ϕ_0 and η_0 have the values of:

$$\phi_0^0 = \begin{Bmatrix} 0 \\ \phi_n^0 \\ \phi_{n+1}^0 \\ \phi_{n+2}^0 \\ 0 \end{Bmatrix} \quad \text{at} \quad t = 0 \tag{53}$$

$$\eta_0^0 = \begin{Bmatrix} 0 \\ \eta_n^0 \\ 0 \end{Bmatrix} \quad \text{at} \quad t = 0 \tag{54}$$

And in a desirable time t_0 followed by $t_0 + \Delta t$:

$$\phi_0^{t_0} = \begin{Bmatrix} .. \\ \phi_n^{t_0} \\ \phi_{n+1}^{t_0} \\ \phi_{n+2}^{t_0} \\ .. \end{Bmatrix} \quad \text{at} \quad t = t_0 \tag{55}$$

$$\eta_0^{t_0} = \begin{Bmatrix} .. \\ \eta_n^{t_0} \\ .. \end{Bmatrix} \quad \text{at} \quad t = t_0 \tag{56}$$

$$\phi_0^{t_0+\Delta t} = \begin{Bmatrix} .. \\ \phi_n^{t_0+\Delta t} \\ \phi_{n+1}^{t_0+\Delta t} \\ \phi_{n+2}^{t_0+\Delta t} \\ .. \end{Bmatrix} \quad \text{at} \quad t = t_0 + \Delta t \tag{57}$$

$$\eta_0^{t_0+\Delta t} = \begin{Bmatrix} .. \\ \eta_n^{t_0+\Delta t} \\ .. \end{Bmatrix} \quad \text{at} \quad t = t_0 + \Delta t \tag{58}$$

Where dots indicate nonzero values.

Specifying the values of ϕ_0 and η_0 for each time step, the relevant values of $(\frac{\partial\phi}{\partial t})_0$ and $(\frac{\partial\eta}{\partial t})_0$ may be simply extracted from dynamic/kinematic boundary conditions. Considering the Bernoulli equation we have:

$$\frac{\partial\phi}{\partial t} = \frac{-1}{2}\left[(\frac{\partial\phi}{\partial x})^2 + (\frac{\partial\phi}{\partial y})^2\right] - gy \tag{59}$$

$$(\frac{\partial\phi}{\partial t})_0 = \\ \frac{-1}{2}\left[\overbrace{(A_0{}^T\phi_0)(\phi_0{}^T A_0)}^{b^2} + \overbrace{(B_0{}^T\phi_0)(\phi_0{}^T B_0)}^{c^2}\right] - g\eta_0 \tag{60}$$

In which:

$\phi_0 = \phi_{0element}$, $\eta_0 = \eta_{0element}$

Applying the kinematic boundary condition together with Figure 4, it can be concluded that:

$$\frac{\partial\eta}{\partial x} = \frac{\eta_i - \eta_j}{TE} = K \tag{61}$$

Therefore for each boundary piece:

$$(\frac{\partial\eta}{\partial x})_0 = bK - c = const \tag{62}$$

Also as it was mentioned, $\Delta\phi$ and $\Delta\eta$ give zero values over that boundary. To employ this condition, the program considers some zero elements in $\{\Delta u\}$ and in the force vector. On the other hand, in the matrix [K], the relevant values for the nodes locating on the boundary are initially set to zero, then the diagonal elements give the value of unity.

3. ITERATION PROCESS

Figure 6 shows the process of iterations. The superscripts indicate that the relevant values belong to the boundary S_4.

Specifying $\{u_o\} = \begin{Bmatrix} \phi_0 \\ \eta_0 \end{Bmatrix}$, the stiffness matrix and the force vector can be computed using 52, after which $\{u_1\}$ may be computed with $\{u_o\}$. Owen, et al [18] have shown that the solution converges when the following condition is satisfied:

$$\frac{\sqrt{\sum_{i=1}^{N} (u_{i_{(r-1)}})^2} - \sqrt{\sum_{i=1}^{N} (u_{i_{(r)}})^2}}{\sqrt{\sum_{i=1}^{N} (u_{i_{(1)}})^2}} \times 100 \le \text{RCON} \tag{63}$$

In application, the parameter RCON usually gives the values of unity. After the solution converge for a certain time step, the program considers $\{u_r\}$, which is the solution of that step, as the initial value for the next step.

$$\begin{array}{ll} t_o & u_o^{t_o} \\ t_o & u_o^{t_o} + \Delta u = u_1^{t_o} \\ t_o & u_1^{t_o} + \Delta u = u_2^{t_o} \\ t_o & u_2^{t_o} + \Delta u = u_3^{t_o} \\ \cdots & \cdots\cdots\cdots \\ \cdots & \cdots\cdots\cdots \\ t_o & u_{r-1}^{t_o} + \Delta u = u_r^{t_o} \\ & \text{solution converged} \\ t_o + \Delta t & u_o^{t_o+\Delta t} = u_r^{t_o+\Delta t} \end{array}$$

Figure 6. The iteration process.

3.1. Forces and Moments

After the velocity potentials are computed for nodal points, the pressure may be computed for the nodes locating in contact with the wall, applying the Bernoulli equation as follows:

$$\frac{p}{\rho} = -gz - \frac{\partial\phi}{\partial t} - \frac{1}{2}\left[\left(\frac{\partial\phi}{\partial x}\right)^2 + \left(\frac{\partial\phi}{\partial y}\right)^2 \right] \tag{64}$$

$$\frac{p}{\rho} = -gz - \left[\frac{2}{\Delta t}\Delta\phi - \left(\frac{\partial\phi}{\partial x}\right)_0 \right] - \frac{1}{2}\left[\overbrace{(A_0{}^T\phi_0)(\phi_0{}^T A_0)}^{b^2} + \overbrace{(B_0{}^T\phi_0)(\phi_0{}^T B_0)}^{c^2} \right] \tag{65}$$

Finally, the forces and moments can be computed integration:

$$F = \int_{-h}^{h} p(x,y,t)\,dy \tag{66}$$

$$M = \int_{-h}^{h} (h+y)\,p(x,y,t)\,dy \tag{67}$$

4. DISCUSSION AND EVALUATION OF RESULTS

In this section, several examples are solved by the program. The parameters required before the execution are:

a = The wave amplitude (m)
h = The depth of still water (m)
T = The wave period (s)
DT = The time increment (s)
TE = The base length of rectangular element (m)

4.1. The Effect of Wave Amplitude

As the first set of examples, the values of forces and moments on the wall are computed for 12 distinct cases, in which h = 5, T = 8, DT = 0.1 and TE = 1.

A summary of outputs are compared with those of Sainflou's Formula modified by Miche-

Rundgren (MR, S, [4]) (Table 1).

The variation of forces and moments with time is shown in Figures 7 to 9.

Finally, outputs are compared with the existing data in Figures 10 and 11. The results show more agreement with (MR and S) in comparison with the outputs of Nagai. Note that (MR and S) have used higher order methods.

The following results can be obtained from the previous figures:

- As a confirmation of the program, the lower the wave amplitude, the lower differences observed between the forces (developed by the wave) and relevant hydrostatic values, as well as moments and hydrostatic ones.
- The maximum values show much variance with respect to the hydrostatic one. This is due to the first and second powers of depth, which are arisen during integration of forces and moments respectively.
- The force and moments increase due to an in increase in wave amplitude.

4.2. The Effect of Wave Period The Parameters assumed for the second set of examples are: h = 15, a = 2, DT = 0.1, TE = 1 and $H_i/h = 0.267$. A summary of outputs are illustrated in Table 2.

Nagai's outputs are approximate results, which are attained comparing the experimental data with the nearest relevant theoretical ones. The results obtained near the wave-breaking zone are not valid. Also the outputs of the program at such zones show relatively high peaks as shown in Figures 12 and 13 for T = 3.

Therefore performing enough examples, a design curve may be extracted as the envelope of this breaking zone (which occurs about T = 4 in this example). After the breaking-zone the outputs show more reliability and well agreement with (MR and S) results (with about 0.5 % error), while Nagai's results show about 20 % deviation with this outputs (Figure 5). The figure states; as the period increases, the forces increase, directly.

4.3. The Sensitivity of Outputs to Time Increment A sensitivity analysis is carried out to show the effect of time increments on the maximum forces and moments. For all of 15 examples here, h = 5, T = 1, a = 1 and TE = 1. A summary of outputs is presented in Table 3. To attain the generality of the problem, another set of examples is solved assuming h = 5, T = 2, a = 1.25 and TE = 1.

From these two examples, the following results can be obtained:

TABLE 1. The Values of Maximum Force and Moment for Various Wave Amplitudes.

			MR and S	MR and S	Nagai	P-RES	P-RES
a_i	$\frac{H_i}{h_i}$	$\frac{H_i}{gT^2}$	F_{total}	M_{total}	F_{total}	F_{total}	M_{total}
0.05	0.02	1.59 E-4	127.5	216.4	127.7	125.9	213.0
0.1	0.04	3.18 E-4	132.5	228.7	133.1	134.4	222.2
0.2	0.08	6.37 E-4	140.1	253.2	144.4	144.7	242.0
0.3	0.12	9.56 E-4	149.4	276.2	156.3	153.7	264.3
0.4	0.16	1.27 E-3	157.5	299.7	156.3	163.6	290.1
0.5	0.20	1.59 E-3	172.2	357.3	182.1	174.7	320.0
0.6	0.24	1.91 E-3	185.2	394.0	196.0	187.2	354.4
0.7	0.28	2.23 E-3	97.72	432.0	210.5	201.1	395.3
0.8	0.32	2.55 E-3	213.1	465.1	220.8	216.7	442.9
0.9	0.36	2.87 E-3	225.2	534.9	241.7	234.9	498.5
1.0	0.40	3.18 E-3	240.2	591.3	258.3	252.2	568.5
1.1	0.44	3.51 E-3	254.8	651.3	275.6	259.3	643.3

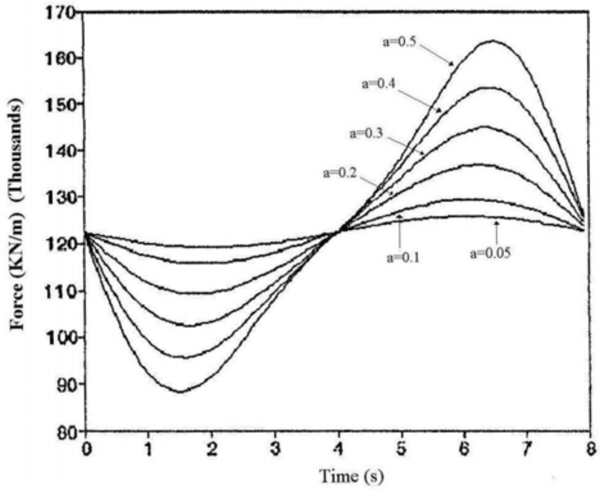

Figure 7. The variation of force with the time (a = 0.05-0.5).

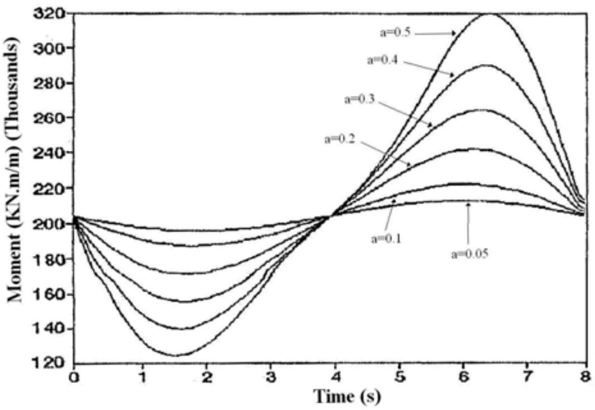

Figure 8. The variation of moment with the time (a = 0.05-0.5).

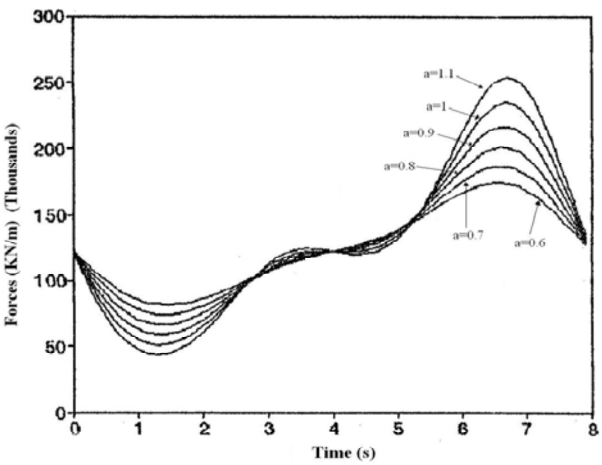

Figure 9. The variation of force with the time (a = 0.6-1.1).

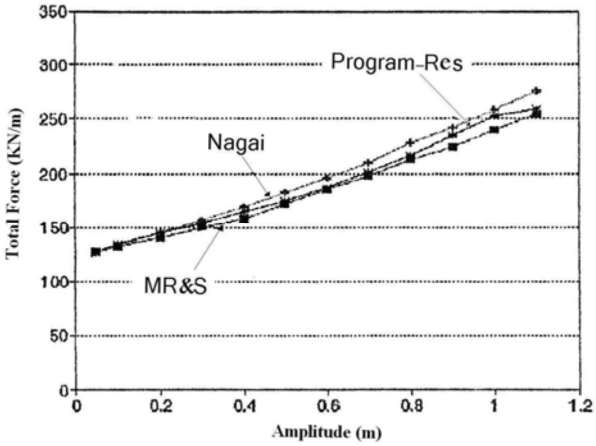

Figure 10. The variation of force with respect to amplitude.

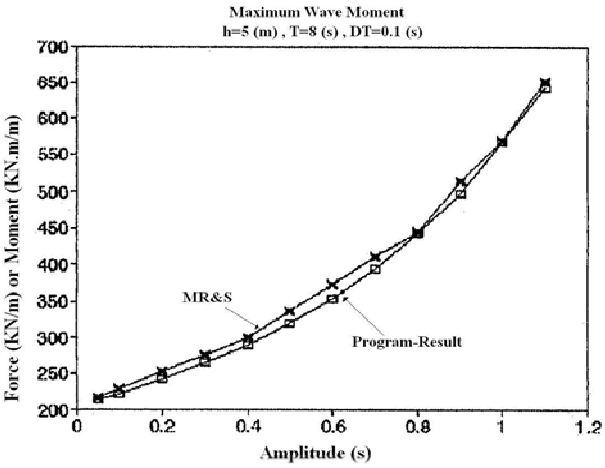

Figure 11. The variation of moment with respect to amplitude.

- The time increment should be chosen such that the value $T/\Delta t$ falls below 5.
- The moments are much sensitive than forces.

4.4. The Effect of Water Depth Here a set of examples is solved for various depth conditions in which T = 5, a = 5 and DR = 0.1. Let's define the relative force and moment as:

$$F_{rel} = F_{wave} / \gamma h^2 \tag{68}$$

TABLE 2. The Force and Moments for Various Wave Periods.

			P-RE	P-RE	P-RE	P-RE	MR and S	MR and S	Nagai
T	$\frac{H_i}{gT^2}$	$\frac{h}{L}$	F_{total}	M_{total}	F_{wave}	M_{wave}	F_{total}	M_{total}	F_{total}
3	0.045	1.07	1554	13470	451.6	7958	-	-	1111.8
4	0.0255	0.601	1352	9030	250.1	3518	-	-	1179.8
5	0.0163	0.390	1372	8703	269.5	3191	-	-	1263.1
6	0.113	0.282	1420	8883	317.7	3371	1395	8882.1	1493.6
7	0.0083	0.222	1464	9094	365.6	3581	1462.3	9091.5	1553.9
8	0.0064	0.183	1500	9283	402.5	3770	1487.7	9282.0	1598.6
9	0.0050	0.157	1530	9461	432.0	3949	1529.4	9459.5	1631.5
10	0.0041	0.137	1557	9627	460.0	4115	1555.2	9625.2	1656.1

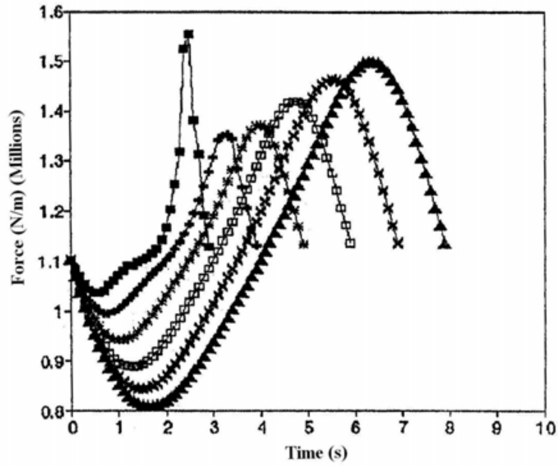

Figure 12. The variation of force with time for different periods.

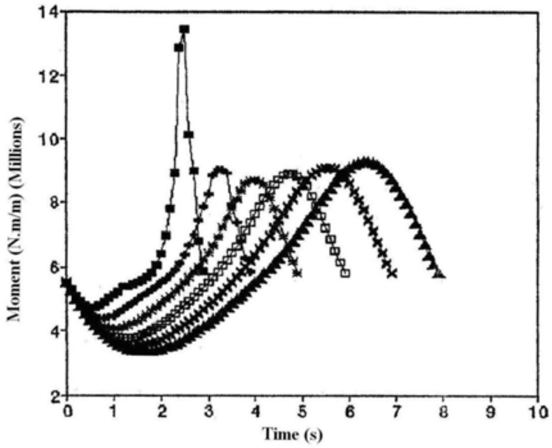

Figure 13. The variation of moment with time for different periods.

TABLE 3. Computational Errors Produced by Various Time Increments.

Δt	$\frac{T}{\Delta t}$	Force Error %	Moment Error %
3	1.67	28.68	43.64
2	2.5	0.1254	0.2159
1	5	0.1254	0.2159
0.9	5.56	9.067	15.08
0.8	6.25	0.1254	0.2159
0.7	7.14	1.395	2.394
0.6	8.33	1.395	2.394
0.5	10	0.1254	0.2159
0.4	12.5	0.1254	0.2159
0.3	16.67	1.183	2.031
0.2	25	0.1254	0.2159
0.1	50	0.1254	0.2159
0.08	62.5	0.06328	0.1092
0.06	83.33	0.04128	0.7111
0.05	100	0.0	0.0

$$M_{rel} = M_{wave} / \gamma h^3 \tag{69}$$

A summary of outputs for forces and moments is illustrated in Figures 14 to 18. The distribution of wave Pressure for different depths is shown in Figures 19 and 20. Values of forces and moments for different depth conditions are presented in Table 4.

These figures show that, as the water depth increases, the forces and moments increase as well. While the values of relative force/moment decrease. Figures 18 to 20 also indicate that the wave pressures change adversely as the water depth varies (note that the resultant force increases as the water depth increases).

4.5. Design Curves (for $H_i / h_i = 0.4$) Here a set of examples is solved in order to acquire a dimensionless design curve such a design curve

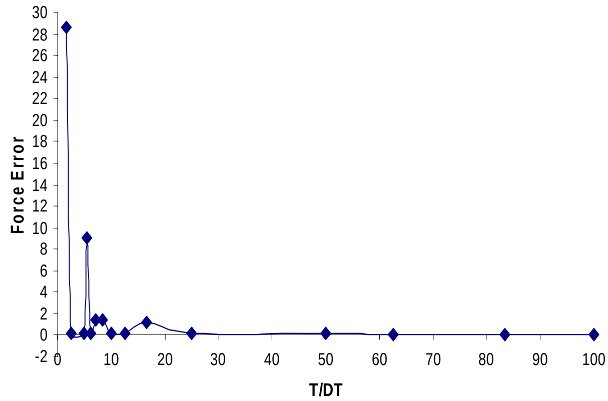

Figure 14. Force error versus $\frac{T}{\Delta T}$.

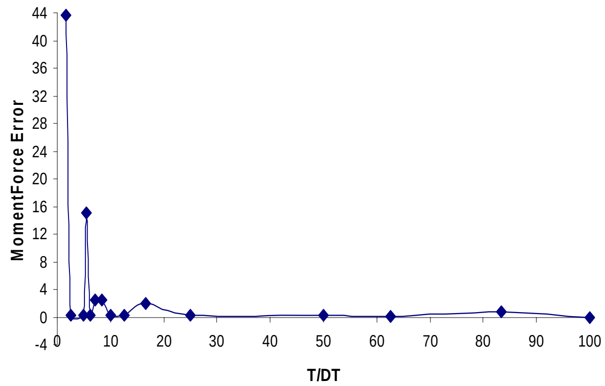

Figure 15. Moment error versus $\frac{T}{\Delta T}$.

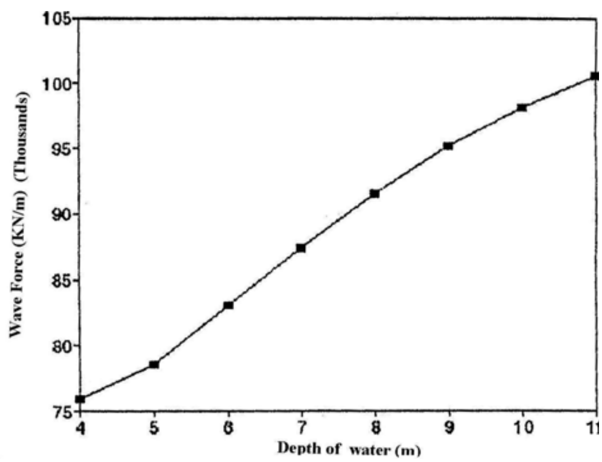

Figure 16. Variation of wave force due to the water depth.

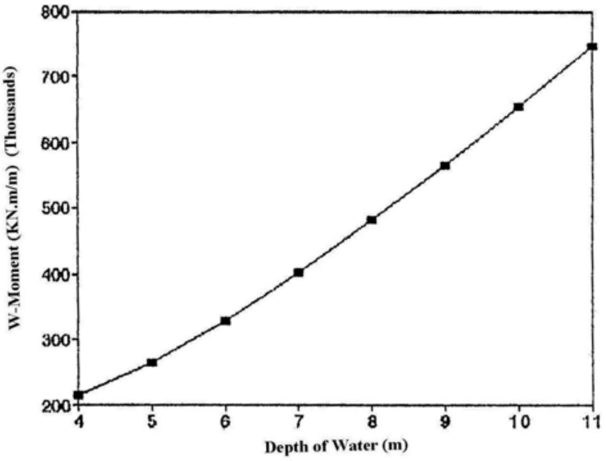

Figure 17. Variation of wave moment due to the water depth.

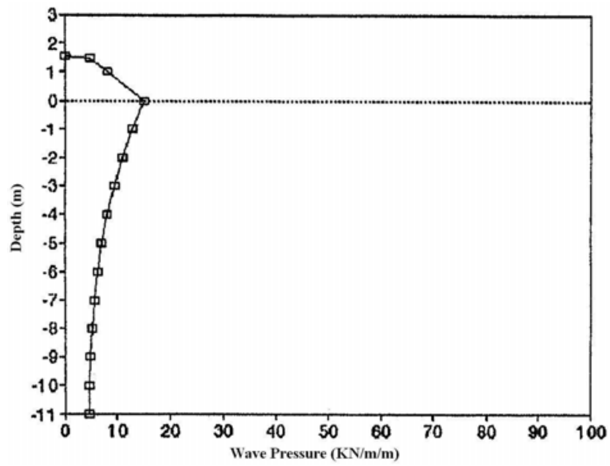

Figure 20. The net pressure of the wave for h = 11.

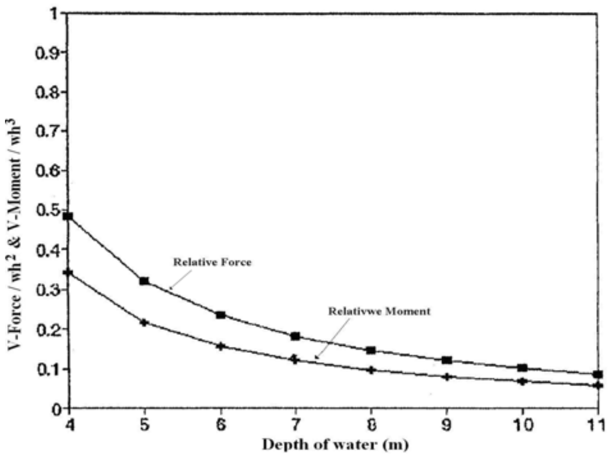

Figure 18. Variation of maximum relative force/moment with respect to the water depth.

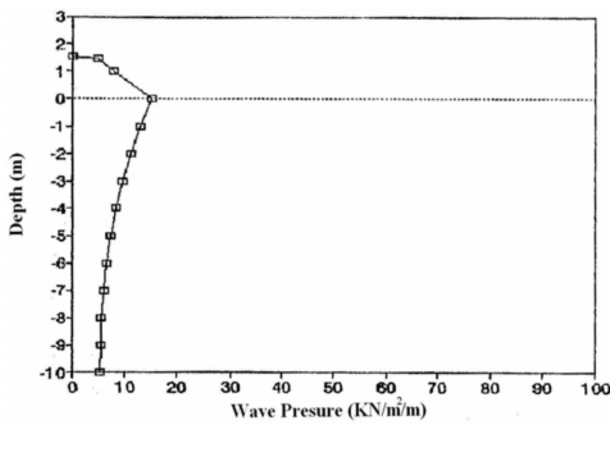

Figure 19. The net pressure of the wave for h = 10.

(Figure 21) is extracted from the data in Table 5.

The parameters assumed here are: h = 4, a = 0.8, DT = 0.1 and TE = 1.

5. SUMMARY AND CONCLUSION

The outputs obtained from the model shows that the effects of wave amplitude in the present study are in agreement with the wave behavior. When the wave amplitude is relatively small, as the force history passes the hydrostatic point, no distinct local maximum/minimum point can be observed. In case of higher amplitudes, however, a distinct local maximum/minimum point can be observed just when the curve passes the hydrostatic Point. Therefore the theories of limited amplitudes, rule such problems where the profiles come out the sinusoidal shapes. In some cases a small depression may be developed at the wave crest, as well as a small knob at the perigee. The outputs (forces and moments) show about 6 % difference with Nagai's experimental data [1].

The results obtained for the effect of period agrees with data obtained by Nagai [1], with about 4 percent difference. The breaking-zone and the envelope of this zone can simply be discretized in the figures.

The moment's sensitivity to time increments is more than the relevant forces. Where $\Delta t < 0.2$ s, the computational error is negligible.

TABLE 4. Values of Forces and Moments for Different Depth Conditions.

Depth	F_{total}	M_{total}	F_{wave}	M_{wave}	F_{rel}	M_{rel}
4	154.30	319.68	75.898	215.14	0.48404	0.34302
5	200.99	468.71	78.487	264.54	0.32036	0.21595
6	259.50	682.26	83.100	329.46	0.23554	0.15564
7	327.55	961.90	87.449	401.66	0.18211	0.11949
8	405.12	1317.2	91.522	480.90	0.14592	0.09584
9	429.07	1756.6	95.166	656.91	0.11989	0.07921
10	588.15	2287.7	98.153	654.34	0.10016	0.06677
11	693.45	2919.5	100.55	755.12	0.08480	0.05716

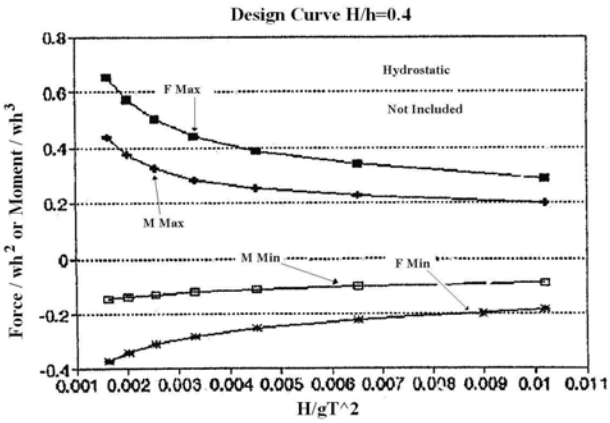

Figure 21. Design curves for $H_i / h_i = 0.4$.

TABLE 5. Dimensionless Values of Forces and Moments for $H_i / h_i = 0.4$.

PERIOD	$\frac{H_i}{gT^2}$	MAX RTL-FRC	MAX RLT-MOM	MIN RTL-FRC	MIN RLT-MOM
4	0.010194	0.28894	0.19971	-0.18326	-0.08737
5	0.006524	0.34051	0.22391	-0.22265	-0.10056
6	0.004531	0.38908	0.25098	-0.25411	-0.11090
7	0.003329	0.44310	0.28508	-0.28367	-0.12035
8	0.002548	0.50466	0.32697	-0.31287	-0.12926
9	0.002014	0.57594	0.37827	-0.34232	-0.13765
10	0.001631	0.65839	0.44054	-0.37173	-0.14535

The outputs of the last set of examples indicate that as the water depth increases, the effect of wave on the lower part of the wall decreases and by comparing the experimental data, In a short, the Program or the numerical model can be used to study the effect of wave under various conditions.

Appendix I. The flow chart of the finite element program is shown in Figure 22.

6. REFERENCES

1. Nagai, S., "Pressure of Standing Wave on Vertical Wall", ***J. Fluid. Mech***., Vol. 95, (1969), 53-76.
2. Tadjbakhsh, I. and Keller, J. B., "Standing Surface

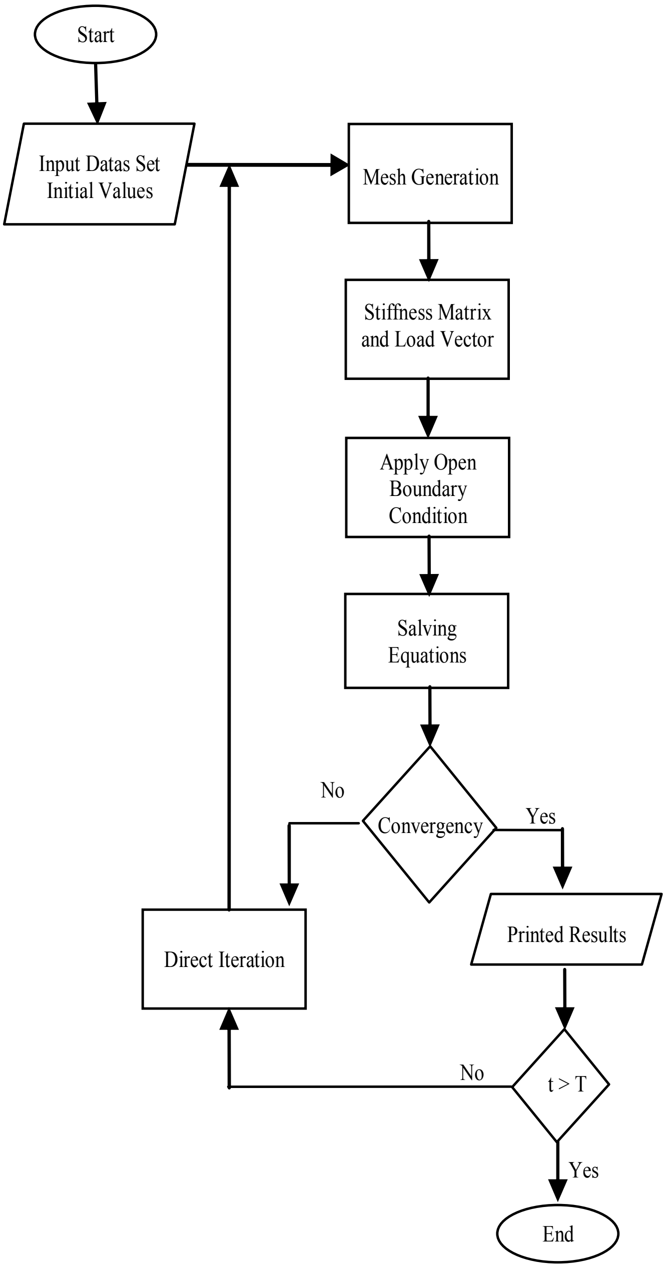

Figure 22. The flow chart of the finite element program.

Waves of Finite Amplitude", ***J. Fluid Mech***., Vol. 8, (1960), 442-451.
3. Goda, Y., "The Fourth Order Approximation to the Pressure of Standing Waves", ***Coastal Engineering in Japan***, Vol. 10, (1967), 1-11.
4. Sainflous and Rundgen, M., "Water Wave Forces", Bulletin Royal Institute of Technology, Stockholm, Sweden, Vol. 54, (1958).
5. Tsuchiya, Y. and Yamaguchi, M., "Limiting Condition for Standing Wave Theories by Perturbation Methods", ***Proceeding of the 12th International Conference on Coastal Engineering***, Vol. 99, (1980), 33-52.
6. Hsu, J. R. C., Tsuchiya, Y. and Silvester, R., "Third-Order Approximation to Short-Crested Waves", ***J. Fluid Mech***., Vol. 90, (1979), 179-196.
7. Roberts, A. J., "Highly Nonlinear Short-Crested Water Waves", ***J. Fluid Mech***., Vol. 135, (1983), 301-321.
8. Roberts, A. J. and Schwartz, L. W., "The Calculation of Nonlinear Short-Crested Waves", ***Physics of Fluids***, Vol. 26, (1983), 2388-2392.
9. Battjes, J. A., "Effect of Short-Crestedness on Wave Loads on Long Structures", ***Applied Ocean Research***, Vol. 4, (1989), 165-172.
10. Clark, P. J., "The Application of Finite Element Analysis to the Solution of Stokes Wave Diffraction Problems", ***Int. J. Num. Meth. Fluids***, Vol. 12, (1991), 345-367.
11. Liao, S. J., "A General Numerical Method for the Solution of Gravity Waves in Shallow Water'', ***Int. J. Num. Meth. Fluids***, Vol. 12, (1991), 727-745.
12. Cao, Y., "Three Dimensional Design Aroused Boundary Integral Methods for Potential Problems", ***Int. J. Num. Meth. Fluids***, Vol. 12, (1991), 785-803.
13. Cao, Y. and Beck, R., "Numerical Computations Two Dimensional Solitary Waves Generated by Moving Disturbances", ***Int. J. Num. Meth. Fluids***, Vol. 17, (1993), 905-920.
14. Johnson, K., "Simulation of Impacts of Fluid Free Surfaces with Solid Boundaries", ***Int. J. Num. Meth. Fluids***, Vol. 19, (1994), 153-176.
15. Takikawa, K., "Numerical Analysis of Finite Amplitude Waves and a Moored Floating Body under Severe Storm Conditions", ***Int. J. Num. Meth. Fluids***, Vol. 21, (1995), 295-310.
16. Washizu, K., "Some Finite Element Techniques for the Analysis of Nonlinear Sloshing Problems", ***Finite Elements n Fluids***, Vol. 5, (1984), 357-376.
17. Luck, J. C., "A Variational Principle for a Fluid with a Free Surface", ***J. Fluid Mech***., Vol. 27, (1967), 395-397.
18. Owen, D. R. J. and Hinton, E., "Finite Element in Plasticity", Pine Ridge Press, Swansea, UK., (1986).